Research Article | Vol. 26, No. 24 | 26 Nov 2018 | OPTICS EXPRESS 31129
Optics EXPRESS

Unidirectional single-frequency operation of a continuous-wave Alexandrite ring laser with wavelength tunability

XIN SHENG,[1,*] GORONWY TAWY,[1] JUNA SATHIAN,[1] ARA MINASSIAN,[2] AND MICHAEL J. DAMZEN[1]

[1]*Photonics Group, The Blackett Laboratory, Dept. of Physics, Imperial College London, Prince Consort Rd. London SW7 2AZ, UK*
[2]*Unilase Ltd, 1 Filament Walk, Unit G02, London, SW18 4GQ, UK*
[*]*xin.sheng14@imperial.ac.uk*

Abstract: High resolution spectroscopy, metrology and quantum technologies (e.g. trapping and cooling) require precision laser sources with narrow linewidth and wavelength tunability. The widespread use of these lasers will be promoted if they are cost-effective, compact and efficient. Alexandrite lasers with a broad tuning band pumped efficiently by low-cost red diodes are a potential candidate, but full performance as a precision light source has not been fully achieved. We present in this work the first continuous-wave (CW) and single-frequency operation of a unidirectional diode-end-pumped Alexandrite ring laser with wavelength tunability. An ultra-compact bow-tie ring cavity is developed with astigmatic compensation and a novel 'displaced mode' design producing CW output power > 1 W in excellent TEM_{00} mode ($M^2 < 1.2$) when using a low brightness pump ($M^2 \geq 30$). Wavelength tuning from 727 - 792 nm is demonstrated using a birefringent filter plate. This successful operation opens the prospects of precision light source applications.

1. Introduction

With the development of the high power red-diode laser, diode-pumped Alexandrite (Cr^{3+}:$BeAl_2O_4$) lasers have become more widely investigated [1–13]. The relatively high absorption coefficient in the spectral region of red diodes guarantees sufficiently high absorption for the gain medium and a small quantum defect between pump and laser photons [6]. The Alexandrite laser, as an alternative to the Ti:sapphire laser, has a broad emission band (701-858 nm) [14,15] and its long upper state lifetime (260 μs at room temperature) [16] enables good energy storage potential for Q-switching. Excellent thermo-mechanical properties including high thermal conductivity (23 $Wm^{-1}K^{-1}$) and high fracture resistance, allow high power operation of Alexandrite [16]. Scheps et al. demonstrated the first diode-pumped Alexandrite laser in 1990 [1] and subsequently achieved 25 mW output power with a slope efficiency of 28% in 1993 [2]. Output power of 1.3 W with 24.5% slope efficiency was achieved under diode-bar-pumping in 2005 [3]. A high brightness tapered diode laser (TDL) was utilized as pump and achieved 200 mW output power with a slope efficiency of 38% in 2013 [4]. In 2014, a diode-end-pumped Alexandrite laser was operated to obtain multi-ten watt (> 26 W) continuous-wave (CW) output power with a slope efficiency of 49% [6]. Diode end-pumped Alexandrite produced a TEM_{00} mode with a slope efficiency of 54% in 2018, which is the highest slope efficiency diode-pumped Alexandrite laser to date [10]. These and other studies have shown that diode-pumping of Alexandrite lasers is a promising route to compactness, simplicity, low cost and high efficiency.

It would be desirable for diode-pumped Alexandrite lasers to have narrow linewidth, controlled wavelength tunability and high output power to enable a multitude of precision

#342088 https://doi.org/10.1364/OE.26.031129
Journal © 2018 Received 10 Aug 2018; revised 4 Oct 2018; accepted 5 Oct 2018; published 12 Nov 2018

Optics EXPRESS

applications, including light source for LIDAR [17–20], high-resolution spectroscopy [21] and quantum technology applications [22]. Flash-lamp-pumped Q-switched unidirectional Alexandrite ring lasers when injection seeded by Ti:sapphire or diode lasers were developed for Lidar or spectroscopy applications [17–21], but the overall laser systems were complex, bulky and low in efficiency. Recently, a Q-switched bi-directional Alexandrite ring laser [12] and a Q-switched ring system in unidirectional single-longitudinal mode operation achieved by injection seeding under pulsed diode-pumping have been developed for LIDAR applications [13].

In this paper, we report the successful demonstration of a unidirectional single-frequency wavelength-tunable CW Alexandrite ring laser under continuous diode-pumping at 638 nm with an ultra-compact design. Developments and results of the unidirectional Alexandrite ring system are described in detail. In Section 2, to assess the potential of Alexandrite Brewster-cut rod, we present results from a compact linear cavity design producing 1.7 W CW output power from 5.4 W pump power and with a slope efficiency of 36.3%. In Section 3, we describe a bow-tie ring cavity design with an Alexandrite Brewster-cut rod with astigmatic compensation. Single-frequency emission is demonstrated from unidirectional operation of the ring laser by employing an optical diode (a Faraday rotator combined with a half-wave plate) to prevent formation of spatial hole burning that would otherwise arise from the standing-waves in a bi-directional cavity. Single frequency output with CW power in excess of 1 W at emission wavelength of 752 nm is demonstrated in a TEM_{00} mode with $M^2 < 1.2$. Wavelength tuning from 727 to 792 nm is achieved using a birefringent filter (BiFi) plate. In section 4, the results of the unidirectional ring cavity design of this paper are summarised, and some of the potential strategies are highlighted for further optimisation and development of the diode-pumped Alexandrite ring laser with narrowband, stabilised wavelength tunability and higher power operation.

2. Compact linear diode-end-pumped Alexandrite laser

Prior to ring laser operation, this section describes an initial study of a diode-end-pumped Brewster-cut Alexandrite crystal using a compact linear laser cavity to assess the power and efficiency potential. Figure 1 is the schematic of the compact diode-pumped Alexandrite laser. A *c*-cut Alexandrite rod with Brewster-angled end faces was used with a length of 8 mm, a diameter of 4 mm and Cr^{3+} doping concentration of 0.22 at.%. The Alexandrite crystal was mounted in a water-cooled copper heat-sink with its *b*-axis and Brewster faces orientated horizontally in a plane-plane compact linear cavity. The absorption coefficient of the Alexandrite rod was measured to be 6.6 cm^{-1} with a He-Ne laser (633 nm). The crystal temperature was maintained at 20°C. The compact linear cavity with a cavity length of 13 mm was formed using two plane mirrors: a dichroic back mirror (BM) which was highly-transmitting (R < 0.2%) for pump (~638 nm) and highly-reflecting (R > 99.9%) at laser wavelength (~755 nm), and an output coupler (OC) with a reflectance of 98.8% at the laser wavelength.

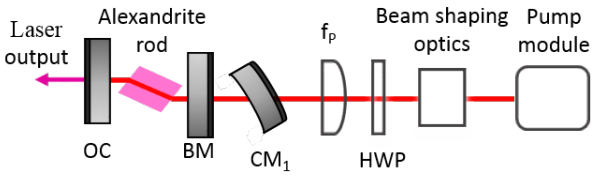

Fig. 1. Schematic of diode-pumped Alexandrite Brewster-cut rod with compact linear laser cavity. BM is a dichroic back mirror, OC is an output coupler with R = 98.8%, f_p is an aspheric pump lens with focal length of 50 mm. HWP is a half-wave plate for matching pump polarization to the crystal *b*-axis. (CM_1 is a curved dichroic mirror that will be used when converting to the ring laser.)

Optics EXPRESS

Pumping was achieved with a multi-bar red-diode module, as described previously [6,8,9], operating nominally at central wavelength of 638 nm with bandwidth (FWHM) of 1.5 nm. The diode module is capable of providing 65 W power in CW mode with beam quality factor M^2 ~240 in horizontal (M^2_x) and ~30 in vertical (M^2_y). Beam quality measurement throughout this paper were made using ISO standard D4-sigma method. Due to its highly-multimode character, the pump beam was spatially filtered in the horizontal direction with two square mirrors acting as a slit aperture to allow a control of the beam quality in the horizontal direction, and then reshaped with a cylindrical lens telescope to match the horizontal size and divergence to the vertical direction. Thus, the horizontal M^2_x value can be improved by narrowing the slit aperture but at the expense of decreasing the power.

The pump power of 5.8 W in CW mode with M^2_x ~30 and M^2_y ~30 was available by setting the aperture size to be 1.5 mm. A half-wave plate (HWP) was used to orient the pump light with high polarisation purity of ~99% parallel to the high absorbing *b*-axis of the Alexandrite rod. Pump absorption in the crystal was ~98%. An aspheric pump lens (f_p) with focal length of 50 mm was used to focus the pump beam through a concave-convex mirror (CM_1) to a spot located near the input face of the rod with measured waist radius ω_x ~62 µm and ω_y ~64 µm. The purpose of adding CM_1 with 50 mm radius of curvature in the compact linear laser system was to facilitate later alignment for the 4-mirror bow-tie ring cavity, without having to re-adjust the pump beam. CM_1 was highly-transmitting for pump and highly-reflecting at laser wavelength.

Figure 2 shows the results of the output power of the compact linear diode-end-pumped Alexandrite laser versus incident pump power on the crystal.

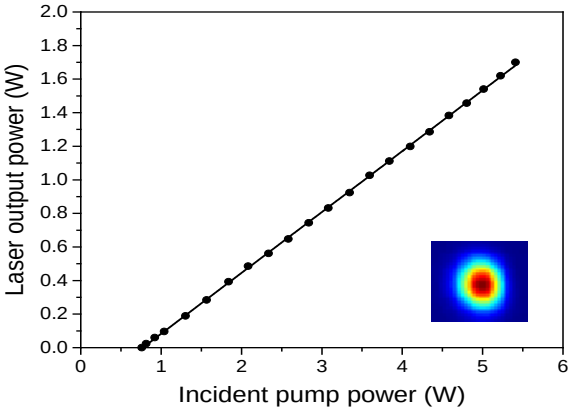

Fig. 2. Laser output power against CW incident pump power for the compact linear diode-end-pumped Alexandrite laser with R = 98.8% Output Coupler. Line is linear fit to the power curve. Inset: Spatial mode profile of the output beam with M^2 = 1.1 at 1.7 W output power.

The slope efficiency was 36.3% and output power of 1.7 W was produced at the incident pump power of 5.4 W, corresponding to an optical-to-optical conversion efficiency of 31.5%. The laser threshold was 760 mW. The inset of Fig. 2 shows the spatial profile of the output of the compact linear cavity. The laser beam had a TEM_{00} beam profile with M^2 value of 1.1 in both x and y directions at maximum pumping power. The spectrum of the Alexandrite laser was centred at a wavelength of ~755 nm.

3. Diode-end-pumped unidirectional Alexandrite ring laser

This section describes an investigation of the diode-end-pumped Alexandrite laser using a bow-tie ring cavity design for single-frequency, tunable and TEM_{00} operation. Figure 3 shows the Alexandrite ring cavity configuration including the Brewster-angle cut crystal as used in the compact linear cavity.

Optics EXPRESS

The 4-mirror bow-tie ring cavity incorporated astigmatic compensation using the two identical curved (concave-convex) mirrors (CM_1 and CM_2) with 50 mm radius of curvature. Mirror CM_1 was presented in the compact linear cavity in Section 2. The folding angles (θ_1, θ_2) of these mirrors was selected as $\theta_1 = \theta_2 = 28°$ to optimize the compensation of the astigmatic distortions introduced by the Brewster-angle cut rod [23,24]. Mirror M_3 was the same as the BM for the compact linear cavity in Fig. 1, OC was an output coupler with a reflectance of 99.0% at the incident angle ($\theta_1/2$) of 14°. The unidirectional operation of the ring laser was achieved by introduction of a TGG Faraday rotator (FR) and a half-wave plate (HWP) to compensate the rotation. A quartz birefringent filter (BiFi) plate with a thickness of 0.5 mm was inserted at Brewster angle to allow wavelength tuning of the output. Our design was configured to have an ultra-compact cavity. The total cavity length was only ~380 mm, and the overall footprint of the laser had dimensions 140 x 90 mm. Here, the crystal temperature was increased to 40°C, as Alexandrite experiences increased performance at elevated temperatures [14,15].

For the pump module, the size of the slit aperture was increased from 1.5 to 2.7 mm, providing an increase in pump power to 10.8 W. The horizontal beam quality of the pump laser increased to M^2_x ~50, while the vertical beam quality remained the same (M^2_y ~30).

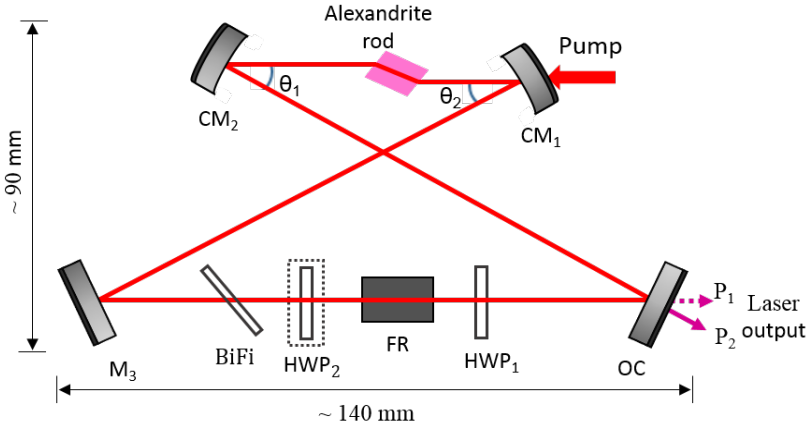

Fig. 3. Schematic of the diode-pumped unidirectional Alexandrite ring laser. CM_1 and CM_2 are curved mirrors. M_3 is a HR mirror for laser. OC is an output coupler with R = 99.0% at the incident angle ($\theta_1/2$) of 14°. The laser wavelength of the unidirectional Alexandrite laser could be tuned using the birefringent filter (BiFi). The unidirectional operation of the ring cavity was achieved using a TGG Faraday rotator (FR) and a half-wave plate (HWP_1). The unidirectional laser output P_1, P_2 could be switched by rotation of the HWP_1. HWP_2 is a second half-wave plate for additional polarization control.

One strategy for TEM_{00} operation of an end-pumped solid state laser is a design to produce a laser mode waist with the size and location to match to the pump beam at the pumped end-face of the crystal, where the majority of the inversion volume is located [6,7,25–27]. In this bow-tie ring cavity, we employed a cavity design using a laser mode waist radius ~20 μm that was significantly smaller than the pump radius ~64 μm but with the waist location displaced from that of the crystal end face. The displaced location of the laser waist was chosen to allow the expansion of the laser mode to match to the pump size at the pumped end-face of the crystal. We denote this as the 'displaced mode' cavity design, as sketched in Fig. 4. The benefit of the 'displaced mode' cavity design with a small waist size (and hence high divergence angle) is that it allows the use of curved mirrors with short radius of curvature, thereby enabling the cavity to be more compact. The pump size cannot be reduced to this small laser waist size due to its high M^2 and its Rayleigh length needing to be matched to the absorption depth (~1.5 mm) of the crystal.

Optics EXPRESS

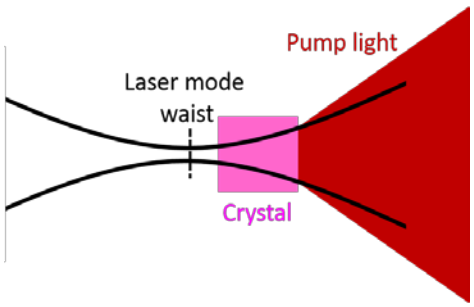

Fig. 4. The 'displaced mode' cavity design concept. The dashed line indicates the location of the laser mode waist in air. The aim of the design is for the expansion of the laser mode to match to the pump beam waist at the pumped end-face of the crystal.

Figure 5(a) shows the results of the unidirectional ring laser output power against incident pump power, without the intracavity BiFi. With pump power of 10.8 W, the unidirectional ring laser produced output power of 1.05 W (in single direction P_2, as shown in Fig. 3). This corresponds to an optical-to-optical conversion efficiency of 9.7% and a laser slope efficiency of 11%. The laser output was in a fundamental TEM_{00} mode with $M^2_x = 1.12$ and $M^2_y = 1.16$, as shown in Fig. 5(b). The inset of Fig. 5(b) shows the spatial profile of the output of the unidirectional Alexandrite ring laser. The lower slope efficiency compared to the compact linear cavity was consistent with the high insertion losses of multiple intra-cavity elements. Small deviations from linearity occurred in the power curve which was attributed to the variation of the laser spatial mode induced by thermal lensing at mid-pumping power.

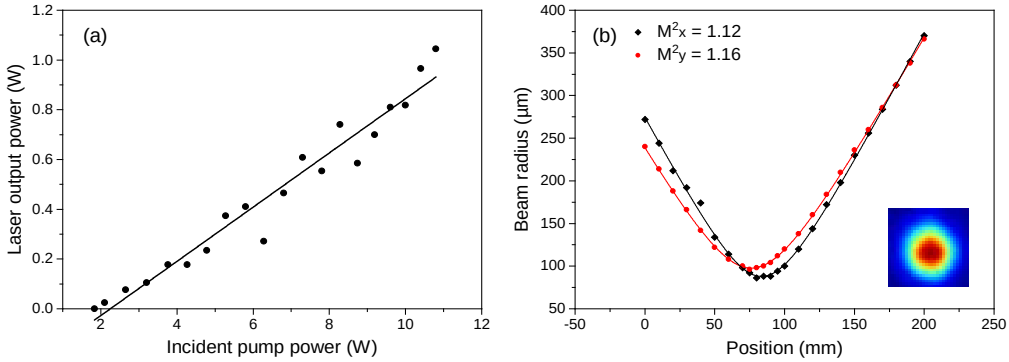

Fig. 5. (a) Laser output power (P_2) against CW incident pump power for the diode-end-pumped unidirectional Alexandrite ring laser with R = 99.0% output coupler under single-frequency operation. Line is linear fit to the power curve. (b) M^2 caustic fit for the single-frequency output of the unidirectional ring laser. Inset: Spatial mode profile of the single-frequency output with $M^2 < 1.2$ at maximum output power (1.05 W).

The spectrum of the laser was investigated by analysing the laser output with a solid Fabry-Pérot (FP) etalon with 6.9 GHz free spectral range and finesse of 50, corresponding to a resolving power ~140 MHz. The ring pattern produced by the interferometer was viewed on a CMOS camera via imaging in the focal plane of an f = 150 mm lens. Single longitudinal mode (SLM) output was achieved in the unidirectional ring laser at emission wavelength of 752 nm, which is seen in Fig. 6 by the single ring pattern (per free spectral range) observed on the etalon. It is noted that the cavity mode spacing of 750 MHz (for the optical path length ~400 mm) was readily resolved by the FP etalon, and the single ring pattern confirmed the single longitudinal mode operation. To the best of our knowledge, this is the first demonstration of unidirectional single-longitudinal mode operation with a CW diode-pumped Alexandrite ring laser. Since the cavity was not stabilised nor narrowed with an etalon, the spectrum could fluctuate and even

Optics EXPRESS

operate on more than single mode on occasion. Further optimization can be expected by adding of an intracavity etalon for enhanced spectral narrowing and a piezoelectric control of cavity length for wavelength stabilisation.

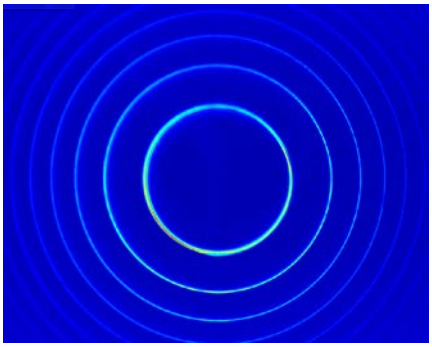

Fig. 6. Spectral ring patterns from a Fabry–Pérot etalon showing single-longitudinal mode operation at output power of 1.05 W and laser wavelength of 752 nm.

A brief investigation was conducted to explore the wavelength tunability of the unidirectional Alexandrite ring laser. Wavelength tuning was achieved by introducing the BiFi plate into the laser cavity and adjusting its angle. In an initial study, the variation of the CW output power as a function of emission wavelength is shown in Fig. 7(a), and in a later implementation in Fig. 7(b). The tuning curves were obtained at maximum pumping power with unidirectional laser output in P_2 direction.

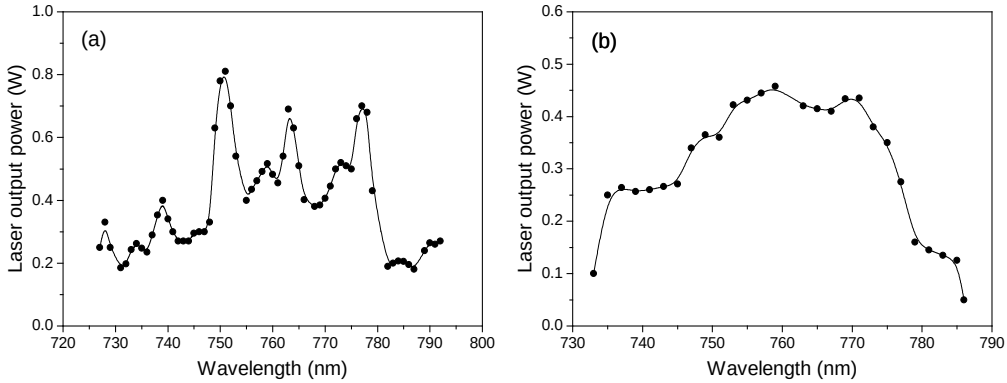

Fig. 7. Wavelength tuning curves for the unidirectional Alexandrite ring laser, (a) using one half-wave plate (HWP_1), and (b) using two half-wave plates (HWP_1 and HWP_2).

In the first study, the unidirectional ring operation was able to be maintained from 727 to 792 nm over a total tuning range of 65 nm, shown in Fig. 7(a). The wavelength tuning curve exhibited modulation with a periodicity of ~12 nm (with 5 main structures peaked at 728, 739, 751, 763, 777 nm). This periodic modulation is consistent with a birefringent filtering effect of the Alexandrite crystal, which rotates the polarization of the intracavity radiation as a function of the wavelength of the laser light when the beam path is not precisely along a crystal principal axis (the *c*-axis in this case). As a result, the intracavity laser light experiences loss from Brewster-cut faces of Alexandrite crystal except when the birefringence acts as an integer-wavelength waveplate, and thereby resulting in the highest power at these discrete wavelengths but preventing a smooth and continuous laser wavelength tuning. A potential reason for the birefringent filtering is that the crystal cut is slightly mismatched with the Brewster cut. By better crystal cut, smoother wavelength tuning should be expected.

Optics EXPRESS

To improve the quality of wavelength tuning with the current Brewster-cut Alexandrite crystal, some compensation was implemented by adding a second half-wave plate (HWP_2) between the FR and the BiFi into the ring cavity, shown in Fig. 3. Figure 7(b) shows the tuning curve for this case. In this instance the wavelength was tuned more smoothly from 733 to 786 nm with considerably reduced modulation, with the polarization of the intracavity light partially able to offset birefringent rotation in the laser crystal, albeit at the expense of lower output power and slightly narrower tuning range.

It is also seen in Fig. 7 that abrupt termination of lasing occurred at the extremes of the tuning range suggesting an extended tuning range appears possible. The tuning range is also partially limited by the reduction of spectral coating performance of intracavity optics on either wavelength side of the Alexandrite's central lasing band ~755 nm. Further long-wavelength extension is also possible by using higher temperature of the Alexandrite crystal [2,3,10].

4. Summary and outlook

We have reported the first demonstration of unidirectional single-frequency operation of a diode-end-pumped Alexandrite ring laser in CW operation with wavelength tunability. Initially, a diode-end-pumped Alexandrite laser using a compact linear cavity design was investigated, CW laser output with power of 1.7 W and slope efficiency of 36.3% in a TEM_{00} beam profile with excellent M^2 value of 1.1 was demonstrated from 5.4 W pump power at 638 nm. Single-frequency output was achieved in the unidirectional ring laser using a bow-tie cavity design with output power in excess of 1 W (1.05 W) at emission wavelength of 752 nm. A slope efficiency of 11% in a TEM_{00} mode with good beam quality $M^2 < 1.2$ was demonstrated. Emission wavelength was tuned between 727 and 792 nm using a birefringent filter (BiFi) plate.

These results show promise for the diode-pumped Alexandrite ring laser in single-frequency operation with tunability. There is clearly scope for further improvement in efficiency, stability and tuning performance, as the investigations were not fully optimized in this work. Further optimization is expected to operate the system with better quality optics and intra-cavity elements with reduced passive insertion loss, and operation at higher temperature for efficiency performance enhancement and extension of tuning range to longer wavelengths [10]. An etalon and a piezoelectric cavity length control can be added for further spectral narrowing and wavelength stabilisation, respectively. The first successful demonstration of the unidirectional single-frequency operation of the wavelength-tunable continuous-wave Alexandrite ring laser opens the way for development of cost-effective and compact laser systems with narrow linewidth, precise wavelength tunability and high power operation in realising applications in areas such as Lidar light source, high-resolution spectroscopy and quantum technology applications.

Funding

Engineering and Physical Sciences Research Council (EPSRC) (EP/R00420X/1); Innovate UK (132531).

Acknowledgments

The authors acknowledge collaboration in this work with M Squared Lasers Ltd. and also acknowledge S. Johnson and M. Kehoe of the Optics Mechanical Workshop at Imperial College London for fabrication of components for the laser work.

References

1. R. Scheps, B. M. Gately, J. F. Myers, J. S. Krasinski, and D. F. Heller, "Alexandrite laser pumped by semiconductor lasers," Appl. Phys. Lett. **56**(23), 2288–2290 (1990).
2. R. Scheps, J. F. Myers, T. R. Glesne, and H. B. Serreze, "Monochromatic end-pumped operation of an Alexandrite laser," Opt. Commun. **97**(5–6), 363–366 (1993).

Optics EXPRESS

3. X. Peng, A. Marrakchi, J. C. Walling, and D. F. Heller, "Watt-level red and UV output from a CW diode array pumped tunable Alexandrite laser," in *Conference on Lasers and Electro-Optics* (Optical Society of America, 2005), paper CMAA5.
4. E. Beyatli, I. Baali, B. Sumpf, G. Erbert, A. Leitenstorfer, A. Sennaroglu, and U. Demirbas, "Tapered diode pumped continuous-wave alexandrite laser," J. Opt. Soc. Am. B **30**(12), 3184–3192 (2013).
5. I. Yorulmaz, E. Beyatli, A. Kurt, A. Sennaroglu, and U. Demirbas, "Efficient and low-threshold Alexandrite laser pumped by a single-mode diode," Opt. Mater. Express **4**(4), 776–789 (2014).
6. A. Teppitaksak, A. Minassian, G. M. Thomas, and M. J. Damzen, "High efficiency >26 W diode end-pumped Alexandrite laser," Opt. Express **22**(13), 16386–16392 (2014).
7. E. Arbabzadah and M. Damzen, "Fibre-coupled red diode-pumped alexandrite TEM_{00} laser with single and double-pass end-pumping," Laser Phys. Lett. **13**(6), 065002 (2016).
8. G. M. Thomas, A. Minassian, X. Sheng, and M. J. Damzen, "Diode-pumped Alexandrite lasers in Q-switched and cavity-dumped Q-switched operation," Opt. Express **24**(24), 27212–27224 (2016).
9. M. J. Damzen, G. M. Thomas, and A. Minassian, "Diode-side-pumped Alexandrite slab lasers," Opt. Express **25**(10), 11622–11636 (2017).
10. W. R. Kerridge-Johns and M. J. Damzen, "Temperature effects on tunable cw Alexandrite lasers under diode end-pumping," Opt. Express **26**(6), 7771–7785 (2018).
11. U. Parali, X. Sheng, A. Minassian, G. Tawy, J. Sathian, G. M. Thomas, and M. J. Damzen, "Diode-pumped Alexandrite laser with passive SESAM Q-switching and wavelength tunability," Opt. Commun. **410**, 970–976 (2018).
12. A. Munk, B. Jungbluth, M. Strotkamp, S. Gaussmann, D. Hoffmann, R. Poprawe, and J. Hoeffner, "Diode pumped Alexandrite ring laser," in *Proc. Advanced Solid State Lasers* (Optical Society of America, 2015), paper ATh2A.46.
13. A. Munk, B. Jungbluth, M. Strotkamp, H.-D. Hoffmann, R. Poprawe, J. Höffner, and F.-J. Lübken, "Diode-pumped alexandrite ring laser in single-longitudinal mode operation for atmospheric lidar measurements," Opt. Express **26**(12), 14928–14935 (2018).
14. J. Walling, O. Peterson, H. Jenssen, R. Morris, and E. O'Dell, "Tunable Alexandrite lasers," IEEE J. Quantum Electron. **16**(12), 1302–1315 (1980).
15. J. W. Kuper, T. Chin, and H. E. Aschoff, "Extended Tuning Range of Alexandrite at Elevated Temperatures," in Advanced Solid State Lasers, Vol. 6 of OSA Proceedings Series (Optical Society of America, 1990), paper CL3.
16. J. Walling, D. F. Heller, H. Samelson, D. J. Harter, J. Pete, and R. C. Morris, "Tunable alexandrite lasers: Development and performance," IEEE J. Quantum Electron. **21**(10), 1568–1581 (1985).
17. V. Wulfmeyer and J. Bösenberg, "Single-mode operation of an injection-seeded alexandrite ring laser for application in water-vapor and temperature differential absorption lidar," Opt. Lett. **21**(15), 1150–1152 (1996).
18. V. Wulfmeyer, "Ground-based differential absorption lidar for water-vapor and temperature profiling: development and specifications of a high-performance laser transmitter," Appl. Opt. **37**(18), 3804–3824 (1998).
19. S. C. Collins, T. D. Wilkerson, V. B. Wickwar, D. Rees, J. C. Walling, and D. F. Heller, "The alexandrite ring laser: A spectrally narrow lidar light source for atmospheric fluorescence and absorption observations," in Advances in atmospheric remote sensing with Lidar, A. Ansmann, R. Neuber, P. Rairoux, and U. Wandinger, ed. (Springer Verlag, Berlin, 1997).
20. X. Chu, "Alexandrite-ring-laser-based Fe Doppler lidar for mobile/airborne deployment," in *Proceeding of the 23rd International Laser Radar Conference* (2006), pp. 385–388.
21. P. Bakule, P. E. G. Baird, M. G. Boshier, S. L. Cornish, D. F. Heller, K. Jungmann, I. C. Lane, V. Meyer, P. H. G. Sandars, W. T. Toner, M. Towrie, and J. C. Walling, "A chirp-compensated, injection-seeded alexandrite laser," Appl. Phys. B **71**(1), 11–17 (2000).
22. S. Burd, D. Leibfried, A. C. Wilson, and D. J. Wineland, "Optically pumped semiconductor lasers for atomic and molecular physics," Proc. SPIE **9349**, 93490P (2015).
23. D. M. Kane, "Ti:sapphire laser cavity mode and pump-laser mode calculations," Appl. Opt. **33**(18), 3849–3856 (1994).
24. H. Kogelnik, E. P. Ippen, A. Dienes, and C. V. Shank, "Astigmatically compensated cavities for CW dye lasers," IEEE J. Quantum Electron. **8**(3), 373–379 (1972).
25. B. Zhou, T. J. Kane, G. J. Dixon, and R. L. Byer, "Efficient, frequency-stable laser-diode-pumped Nd:YAG laser," Opt. Lett. **10**(2), 62–64 (1985).
26. R. A. Fields, M. Birnbaum, and C. L. Fincher, "Highly efficient Nd:YVO_4 diode-laser end-pumped laser," Appl. Phys. Lett. **51**(23), 1885–1886 (1987).
27. D. L. Sipes, "Highly efficient neodymium: yttrium aluminum garnet lasers end pumped by a semiconductor laser array," Appl. Phys. Lett. **47**(2), 74–76 (1985).